RSC Advances

PAPER

View Article Online
View Journal | View Issue

Cite this: *RSC Adv.*, 2019, **9**, 22176

Synthesis and properties of hyperbranched polymers for polymer light emitting devices with sunlight-style white emission†

Yuling Wu, *[ab] Dongyu Wu,[a] Haocheng Zhao,[cd] Jie Li, *[a] Xuefeng Li,[a] Zhongqiang Wang,[a] Hua Wang,[a] Furong Zhu *[b] and Bingshe Xu[a]

A new series of hyperbranched polymers consisting of fluorene-*alt*-carbazole as the branches and the three-dimensional-structured spiro[3.3]heptane-2,6-dispirofluorene (**SDF**) as the core were designed and synthesized by one-pot Suzuki coupling polycondensation. A phosphor group with broad full width at half maximum (FWHM) bis(1-phenyl-isoquinoline)(acetylacetonato)iridium(III) (**Ir(Brpiq)$_2$acac**, 0.08 mol%) as the red-light emitting unit and bis(2-(4-bromophenyl)-1-[6-(9-carbazolyl)hexyl]-imidazole)(2-(5-(4-fluorinated phenyl)-1,3,4-triazole)pyridine)iridium(III) (**(CzhBrPI)$_2$Ir(fpptz)**) as the green-light emitting unit were introduced into the backbones to obtain sunlight-style white-light emission by adjusting the feeding ratios of **(CzhBrPI)$_2$Ir(fpptz)** (0.08 to 0.32 mol%). The results indicate the synthesized polymers show high thermal stabilities and good amorphous film morphology because of the hyperbranched structures. Besides, the lowest unoccupied molecular orbital (LUMO) levels of polymers were reduced and the electron injection was improved because of excellent electron-transporting ability of the triazole unit in the green group. The hyperbranched structures can effectively suppress the polymers' chain distortion and aggregation, and promote the incomplete Förster resonance energy transfer (FRET) efficiency from fluorene-*alt*-carbazole segments to Ir complex units. As a result, the devices with hyperbranched polymer light-emitting layers realize white light emission, and the optimized device also exhibits good electroluminescent (EL) performance with Commission Internationale de l'Eclairage (CIE) coordinates at (0.32, 0.31), a maximum luminance of 9054 cd m^{-2}, a maximum current efficiency of 3.59 cd A^{-1} and a maximum Color Rendering Index (CRI) of 91. The hyperbranched polymers based on fluorene-*alt*-carbazole branches and a **SDF** core and high-efficiency phosphor groups with broad full width at half maximum are attractive candidates for sunlight-style white polymer light-emitting device.

Received 3rd May 2019
Accepted 27th June 2019

DOI: 10.1039/c9ra03307f

rsc.li/rsc-advances

Introduction

Recently, hyperbranched polymers have attracted much attention as light-emitting materials in displays, lighting and other photonic devices because of their unique structures and properties compared to their linear analogues.[1–5] The highly branched structure and a large number of terminal functional units are two important factors of hyperbranched polymers obvious difference from linear polymers.[6–9] Firstly, the hyperbranched polymers with three-dimensional structure can ably restrain the aggregation of polymer chains, make the material form amorphous films of good quality, increase the glass transition temperature (T_g) of the polymers and tune the light emission properties.[10–14] Secondly, they are easy to be prepared by one-pot Suzuki coupling polymerization with similar properties to dendritic polymers or other well defined polymers.[15–17] Meanwhile, white polymer light-emitting devices (WPLEDs) have gained extensive attention owing to their potential applications in solid lighting sources and large-area full-color displays, and they also exhibit great advantages such as high contrast, high stability, low price and easy fabrication process.[18–22] A conventional approach to gain white-light emission is to synthesize a single molecule polymer with blue light emitting groups and complementary orange light emitting units or green and red light emitting units.[23–29] Therefore, in order to obtain the sunlight-style white organic light emitting devices (OLEDs), we introduce broad spectral green and red

[a]*Key Laboratory of Interface Science and Engineering in Advanced Materials, Taiyuan University of Technology, Taiyuan, 030024, China. E-mail: wuyuling@tyut.edu.cn; lijie01@tyut.edu.cn*

[b]*Department of Physics, Institute of Advanced Materials, and Institute of Research and Continuing Education (Shenzhen), Hong Kong Baptist University, Kowloon Tong, Hong Kong, P. R. China. E-mail: frzhu@hkbu.edu.hk*

[c]*Department of Electrical Engineering, Shanxi Institute of Energy, Taiyuan, 030600, China*

[d]*College of Materials Science and Engineering, Taiyuan University of Science and Technology, Taiyuan, 030024, China*

† Electronic supplementary information (ESI) available: ^{1}H NMR and ^{13}C NMR characterization of the complexes and hyperbranched polymers, the PL spectra of green and red phosphor groups. See DOI: 10.1039/c9ra03307f

phosphor light-emitting groups into the hyperbranched polymer.

In this paper, the hyperbranched white light-emitting polymers with 3,6-carbazole-*alt*-2,7-fluorene (**PFCz**) branches, spiro[3.3]heptane-2,6-dispirofluorene (**SDF**) core (10 mol%), and bis(1-(4-bromo phenyl)-isoquinoline)(acetylacetonato)iridium(III) (**Ir(Brpiq)$_2$acac**) and bis(2-(4-bromophenyl)-1-[6-(9-carbazolyl)hexyl]-imidazole)(2-(5-(4-fluorinated phenyl)-1,3,4-triazole)pyridine)iridium(III) (**(CzhBrPI)$_2$Ir(fpptz)**) groups were constructed. For the sake of acquiring white-light emission, the red light-emitting unit **Ir(Brpiq)$_2$acac** with contents of 0.08 mol% and green light-emitting unit **(CzhBrPI)$_2$Ir(fpptz)** with different contents from 0.08 mol% to 0.32 mol% was adopted to develop white polymers, where the full width at half maximum for two phosphor groups is up to 77 nm and 81 nm, respectively. The three-dimensional-structured **SDF** exhibits immense morphological stability and strong fluorescence.[30,31] Moreover, the formed hyperbranched interpenetrating network can prevent rotation of the adjacent aryl groups, and promote the incomplete Förster resonance energy transfer (FRET) from the fluorene-*alt*-carbazole portions to the Ir(III) complex units, to obtain white light emission and further improve the electroluminescent (EL) performance of polymers-based OLEDs.

Experimental section

Materials and characterization

The detailed description about materials and measurements (NMR spectra, elemental analysis, gel permeation chromatography, UV-vis absorption spectra, steady-state emission spectra, excited-state lifetime, thermogravimetric analysis, differential scanning calorimetry, X-ray diffraction, atomic force microscopy, and cyclic voltammetry) can be found in Section S1 in ESI.† And the detailed process about OLEDs fabrication and testing can be found in Section S2 in ESI.†

Syntheses

Spiro[3.3]heptane-2,6-di-(2′,2″,7′,7″-tetrabromospirofluorene) (**TBrSDF**),[32,33] 3,6-dibromo-*N*-(2-ethylhexyl)-carbazole (**DBrCz**),[34,35] and bis(1-(4-bromo phenyl)-isoquinoline)(acetylacetonato)iridium(III) (**Ir(Brpiq)$_2$acac**)[36–38] were synthesized according to the published literature. Synthetic routes of ligands and complexes **(CzhBrPI)$_2$Ir(fpptz)** are displayed in Section S3 and Scheme S1 in ESI.†

General procedure for the synthesis of copolymers PFCzSDF10R8G8–PFCzSDF10R8G32. Under nitrogen protection, a mixture of predetermined amount of the monomers (**DBrCz**, **M2**, **TBrSDF**, (**Ir(Brpiq)$_2$acac**) and **(CzhBrPI)$_2$Ir(fpptz)**) in toluene (30 ml) was joined in an aqueous solution (5 ml) of potassium carbonate (2 M) and a catalytic amount of $Pd(PPh_3)_4$ (2.0 mol%). Aliquat 336 (1 ml) in toluene (5 ml) was added as the phase transfer catalyst. The mixture was vigorously stirred and refluxed at 90 °C for 3 days. Phenylboronic acid was then added to the reaction mixture and stirred at 90 °C for an additional 12 h. Finally, bromobenzene was added in the same way by heating for 12 h again. The reaction mixture was cooled to room temperature and added dropwise to excess methanol. The precipitates were collected by filtration and Soxhlet extracted with acetone for 72 h and then further purification through column chromatography using toluene as the eluent to afford the target hyperbranched polymers.

PFCzSDF10R8G8. **DBrCz** (0.153 g, 0.35 mmol), **M2** (0.354 g, 0.55 mmol), **TBrSDF** (0.071 g, 0.1 mmol), **Ir(Brpiq)$_2$acac** (0.32 ml, 2×10^{-3} mol L^{-1}) and **(CzhBrPI)$_2$Ir(fpptz)** (0.32 ml, 2×10^{-3} mol L^{-1}). Dark green powder, yield: 63.7%. ^{1}H NMR ($CDCl_3$) δ (ppm): 8.53–8.31 (–ArH–), 8.00–7.35 (–ArH–), 4.32–4.15 (–N–CH_2–), 3.42–3.12 (–CH_2–), 2.20–1.89 (–C–CH_2–), 1.22–0.93 (–CH_2–), 0.82–0.58 (–CH_3).

PFCzSDF10R8G16. **DBrCz** (0.153 g, 0.35 mmol), **M2** (0.354 g, 0.55 mmol), **TBrSDF** (0.071 g, 0.1 mmol), **Ir(Brpiq)$_2$acac** (0.32 ml, 2×10^{-3} mol L^{-1}) and **(CzhBrPI)$_2$Ir(fpptz)** (0.64 ml, 2×10^{-3} mol L^{-1}). Green powder, yield: 64.9%. ^{1}H NMR ($CDCl_3$) δ (ppm): 8.53–8.29 (–ArH–), 8.07–7.29 (–ArH–), 4.32–4.14 (–N–CH_2–), 3.46–3.12 (–CH_2–), 2.19–1.87 (–C–CH_2–), 1.22–0.93 (–CH_2–), 0.81–0.50 (–CH_3).

PFCzSDF10R8G24. **DBrCz** (0.153 g, 0.35 mmol), **M2** (0.354 g, 0.55 mmol), **TBrSDF** (0.071 g, 0.1 mmol), **Ir(Brpiq)$_2$acac** (0.32 ml, 2×10^{-3} mol L^{-1}) and **(CzhBrPI)$_2$Ir(fpptz)** (0.96 ml, 2×10^{-3} mol L^{-1}). Green powder, yield: 63.5%. ^{1}H NMR ($CDCl_3$) δ (ppm): 8.52–8.40 (–ArH–), 8.09–7.30 (–ArH–), 4.34–4.10 (–N–CH_2–), 3.47–3.09 (–CH_2–), 2.20–1.87 (–C–CH_2–), 1.22–0.93 (–CH_2–), 0.86–0.52 (–CH_3).

PFCzSDF10R8G32. **DBrCz** (0.153 g, 0.35 mmol), **M2** (0.354 g, 0.55 mmol), **TBrSDF** (0.071 g, 0.1 mmol), **Ir(Brpiq)$_2$acac** (0.32 ml, 2×10^{-3} mol L^{-1}) and **(CzhBrPI)$_2$Ir(fpptz)** (1.28 ml, 2×10^{-3} mol L^{-1}). Dark green powder, yield: 66.5%. ^{1}H NMR ($CDCl_3$) δ (ppm): 8.53–8.28 (–ArH–), 8.09–7.30 (–ArH–), 4.32–4.05 (–N–CH_2–), 3.52–3.16 (–CH_2–), 2.20–1.93 (–C–CH_2–), 1.21–0.94 (–CH_2–), 0.82–0.540 (–CH_3).

Results and discussion

Synthesis and characterization

The synthetic routes and chemical structures of the polymers were shown in Scheme 1, a new series of the hyperbranched polymers based on 3,6-carbazole-*co*-2,7-fluorene branches with **SDF** (10 mol%) as the core were synthesized by one-pot Suzuki coupling polycondensation in relatively high yields. To obtain the better color saturation and sunlight-style white-light emission, the red-light-emitting unit **Ir(Brpiq)$_2$acac** having a broad full width at half maximum up to 77 nm was incorporated into the framework with the feed ratios of 0.08 mol% that the optimum proportion of red light added was obtained through previous studies (Fig. S8, ESI†), where the corresponding hyperbranched polymers with the greed-light-emitting unit **(CzhBrPI)$_2$Ir(fpptz)** of 0.08 mol%, 0.16 mol%, 0.24 mol% and 0.32 mol% are corresponding to **PFCzSDF10R8G8**, **PFCzSDF10R8G16**, **PFCzSDF10R8G824** and **PFCzSDF10R8G32**, respectively. The synthetic and structural results of **PFCzSDF10R8G8–PFCzSDF10R8G32** are summarized in Table 1.

Because of the same feed ratios of monomers **DBrCz**, **M2** and **TBrSDF** for polymers **PFCzSDF10R8G8–PFCzSDF10R8G32**, their

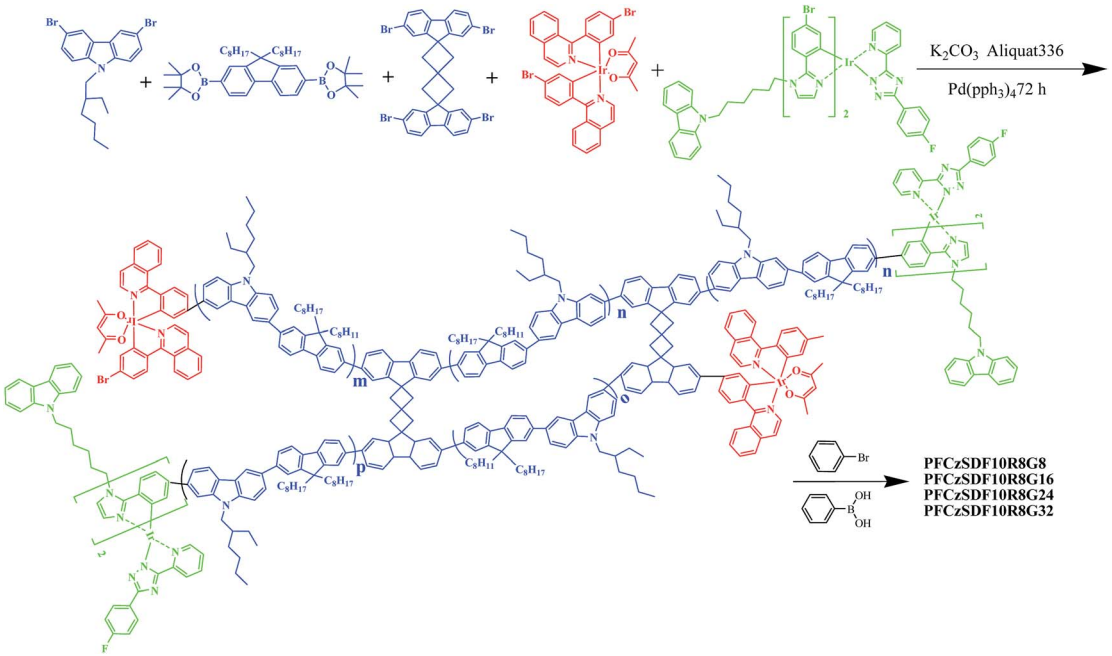

Scheme 1 Synthesis of the hyperbranched polymers.

^{1}H NMR spectra were quite similar (Fig. S6, ESI†). The proton signals of **Ir(Brpiq)$_2$acac** and **(CzhBrPI)$_2$Ir(fpptz)** have little effect because of their low contents, revealing the similar backbone structures for four hyperbranched polymers. The actual ratio of monomers **DBrCz**, **M2** and **SDF** is quite close to the feed ratio by calculating the number of hydrogens at different positions, taking **PFCzSDF10R8G24** as an example (Fig. S7, ESI†). It is noted that the number-average molecular weights (M_n) of the copolymers determined by GPC ranged from 9604 to 10 828 with a polydispersity index (PDI) from 1.79 to 2.09. The resulting hyperbranched polymers are readily soluble in common organic solvents such as $CHCl_3$, THF and toluene.

Structural properties

Powder X-ray diffraction (XRD) measurements judged whether the hyperbranched polymers have an ordered structure. As illustrated in Fig. 1, the polymers had no obvious XRD diffraction peak at small angle and only existed the wide peak around 20° revealed the crosslinking network of the hyperbranched polymers being completely amorphous.

Film morphology

The morphology of the spin-coated films of the hyperbranched polymers was investigated by atomic force microscopy (AFM) at a tapping mode as a key factor for the PLED fabrication and the AFM images of **PFCzSDF10R8G8–PFCzSDF10R8G32** were showed in Fig. 2. Generally, all the films show flat and smooth surface without any pinhole defects. The root-mean-square (RMS) roughness values of hyperbranched polymers are 0.794 nm, 0.864 nm, 0.520 nm, and 0.609 nm, respectively. The results imply that the three-dimensional structured **SDF** branch point and hyperbranched structure can promote the formation of amorphous films with good quality. The uniform amorphous morphology is favorable for PLED fabrication.

Thermal properties

The TGA and DSC data of the hyperbranched polymers are shown in Fig. 3 and Table 2. All of the hyperbranched polymers exhibit good thermal stability with only the small increments of weightlessness being observed before 400 °C, which can be attributed to break away from the solvent molecules in hyperbranched crossover network of polymer, such as methylene

Table 1 Polymerization results and characterizations of the polymers

Copolymers	n_{DBrCz}	n_{M2}	n_{TBrSDF}	n_{Red}	n_{Green}	Yield (%)	GPC	
							M_n	PDI
PFCzSDF10R8G8	0.35	0.55	0.10	8×10^{-4}	8×10^{-4}	63.7	10 593	1.79
PFCzSDF10R8G16	0.35	0.55	0.10	8×10^{-4}	16×10^{-4}	64.9	9604	1.86
PFCzSDF10R8G24	0.35	0.55	0.10	8×10^{-4}	24×10^{-4}	63.5	10 828	2.08
PFCzSDF10R8G32	0.35	0.55	0.10	8×10^{-4}	32×10^{-4}	66.5	10 833	2.09

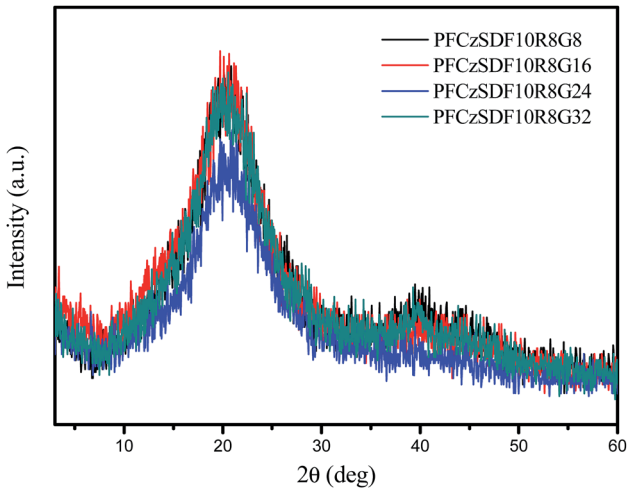

Fig. 1 X-ray powder diffraction pattern of the hyperbranched polymers.

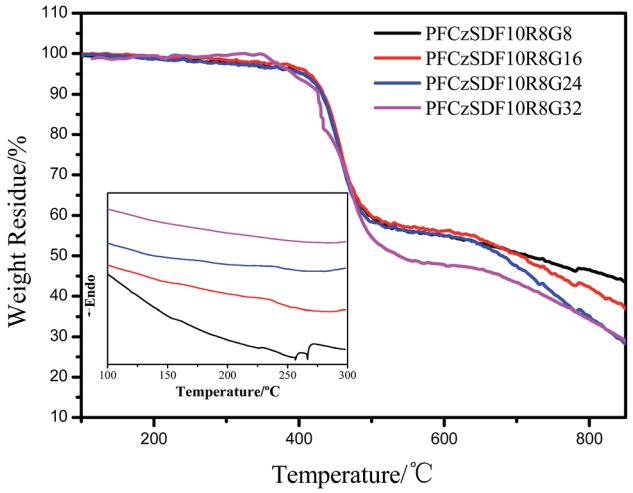

Fig. 3 TGA and DSC (inset) curves of the polymers in nitrogen atmosphere with a heating rate of 10°C min^{-1} and 5 °C min^{-1}, respectively.

chloride, tetrahydrofuran and toluene. The decomposition temperature for the hyperbranched polymers is 410 °C, corresponding a 5% weight loss. The high thermal stability of the hyperbranched polymers is suggested to benefit from the presence of a large amount of carbazole groups, which are known to exhibit excellent thermal and chemical stabilities.[39] Meanwhile, the high thermal stability is a significant characteristic of hyperbranched polymers. The relatively high glass transition temperatures (T_g, inset of Fig. 3) of the copolymers at around 230 °C are found in the DSC curves, which indicates the hyperbranched structures can enhance the thermal stabilities on account of their rigid.

Photophysical properties

The normalized UV-vis absorption and PL spectra of the hyperbranched polymers in dilute solution are shown in Fig. 4a. The absorption bands at around 364 nm are due to the π–π* transitions of poly(fluorene-*alt*-carbazole) backbones,[40] which are blue-shifted about 20 nm compared with the fluorene-based hyperbranched copolymer.[41] This notable hypochromatic shift is attributable to the interruption of the conjugation of the copolymer backbone by the introduction of the 3,6-carbazole linkage.

In the PL spectra, the hyperbranched polymers exhibit emission bands at 420 nm and a slight vibronic shoulder at 440 nm, which can be attributed to 0–0 and 0–1 intrachain singlet transitions in the poly(fluorene-*alt*-carbazole) branches.[42,43] The PL spectra kept in touch with the fluorene-based hyperbranched copolymer,[41] which respect to the blue-shift caused by the (fluorene-*alt*-carbazole) backbones being cancelled out with the red-shift caused by the green phosphor

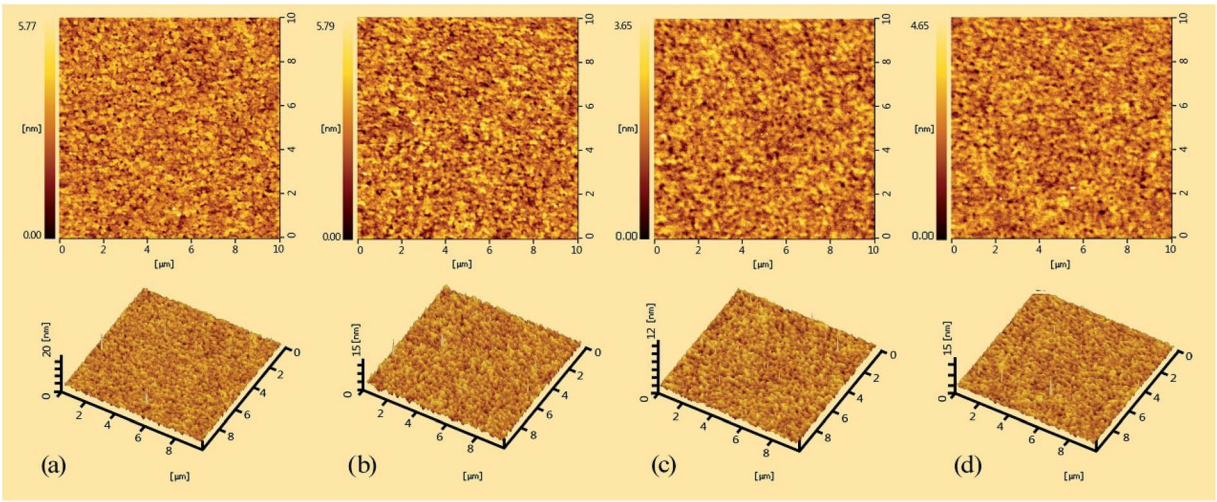

Fig. 2 AFM images (10 × 10 μm) of the hyperbranched polymer films: (a) **PFCzSDF10R8G8**, (b) **PFCzSDF10R8G16**, (c) **PFCzSDF10R8G24** and (d) **PFCzSDF10R8G32**.

Table 2 Thermal and photophysical properties of the copolymers

			Dilute solution		Solid film	
Copolymers	T_d (°C)	T_g (°C)	λ_{abs} (nm)	λ_{PL} (nm)	λ_{abs} (nm)	λ_{PL} (nm)
PFCzSDF10R8G8	417	210	364	420, 440	361	422, 445, 519, 618
PFCzSDF10R8G16	417	228	364	420, 440	360	422, 444, 519, 618
PFCzSDF10R8G24	418	232	365	420, 440	362	422, 445, 519, 618
PFCzSDF10R8G32	408	230	364	419, 439	363	421, 446, 519

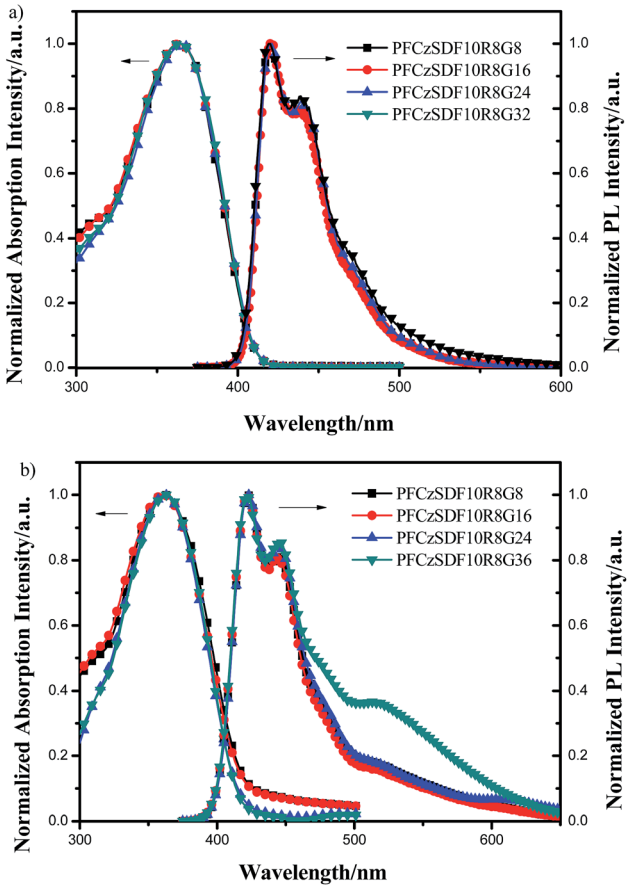

Fig. 4 UV-vis absorption and PL spectra of the hyperbranched polymers: (a) in $CHCl_3$ solution (10^{-5} M) and (b) in solid film.

groups. In order to obtain resembling sunlight white-light emitting, the phosphor group having a broad full width at half maximum were introduced into the hyperbranched polymers backbone, but no distinct absorption or emission peaks of the **Ir(Brpiq)$_2$acac** and **(CzhBrPI)$_2$Ir(fpptz)** (Fig. S8, ESI,† the PL spectra of **Ir(Brpiq)$_2$acac** and **(CzhBrPI)$_2$Ir(fpptz)** respectively located at 613 nm and 508 nm) unit can be observed in the spectra because of its comparatively low contents in the hyperbranched polymers, and the FRET is exclusively intra-chain in dilute solution.

In films, the hyperbranched polymers exhibit UV-vis absorption bands at around 362 nm owning to the π–π* transitions of the poly(fluorene-*alt*-carbazole) backbones (Fig. 4b and Table 2). In the PL spectra, the maximum emission bands of copolymers are at about 422 nm, along with a shoulder at around 445 nm, showing no obvious bathochromic shift with respect to those in dilute solution. In addition, the four polymers all showed small luminescence peaks at 519 nm and 618 nm, which is due to the introduction of green light group **(CzhBrPI)$_2$Ir(fpptz)** and red light group **Ir(Brpiq)$_2$acac**, respectively. For **PFCzSDF10R8G32**, the emission band of **(CzhBrPI)$_2$Ir(fpptz)** centered at 519 nm can be observed and the emission band of to **Ir(Brpiq)$_2$acac** centered at 613 nm cannot be observed which due to the red peak being encased in the green peak as a result of both intra- and interchain FRET from fluorene-*alt*-carbazole unit to **(CzhBrPI)$_2$Ir(fpptz)** unit to **Ir(Brpiq)$_2$acac** unit again.[44–46] This result indicates that the hyperbranched structure can prevent the aggregation of the polymer chains efficiently and promote incomplete FRET efficiency from fluorene-*alt*-carbazole segment to the Ir complex units.

Electroluminescent properties

In order to reveal the EL performance of synthesized polymers, OLEDs with the configuration of ITO/PEDOT:PSS (40 nm)/polymer (50 nm)/TPBi (35 nm)/LiF (1 nm)/Al (150 nm) were fabricated. The device structure and relative-energy-level diagrams for involved devices are shown in Fig. 5a and b, respectively. As mentioned above, the green group **(CzhBrPI)$_2$Ir(fpptz)** incorporated into the backbone can effectively lower the HOMO level and the LUMO level of polymers, and increase their electro-transporting ability. At the same time, the hole-transporting ability of polymers remains almost constant because there are carbazole unit in the polymers main chain and **(CzhBrPI)$_2$Ir(fpptz)**. Here 1,3,5-tris(*N*-phenylbenzimidazol-2-yl)benzene (TPBi) is used as the electron-transport layer to facilitate electron transport as before.[25]

The electroluminescence spectra of the hyperbranched polymers-based OLEDs are shown in Fig. 6 at voltages varying from 6 to 11 V, and the related performance parameters are summarized in Table 3. The main peaks at 420 nm with a shoulder at 440 nm are well corresponding to their PL emission, and the peaks in the long-wavelength around 530 nm and 615 nm are gradually enhanced with increasing the voltages, which are corresponding to the emissions of green-light emission unit **(CzhBrPI)$_2$Ir(fpptz)** and the red-light emission unit **Ir(Brpiq)$_2$acac**, respectively. As a result, **PFCzSDF10R8G8** and **PFCzSDF10R8G16**-based OLEDs both exhibit like white-light

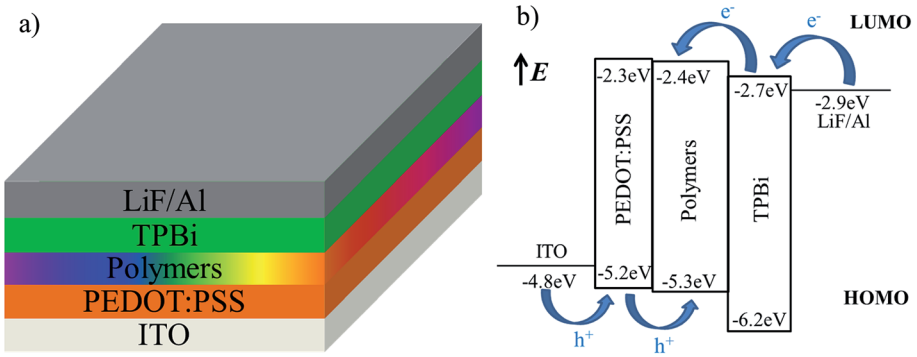

Fig. 5 Device structure (a) and energy-level (b) diagrams of OLEDs.

emission (inset Fig. 6a and b). With the increase of contents of the green-light emission unit **(CzhBrPI)$_2$Ir(fpptz)**, corresponding **PFCzSDF10R8G24**-based device shows a relatively better white emission where the EL spectra contain obviously increased green light emission waveband, displayed in Fig. 6c. What's more, the spectra of **PFCzSDF10R8G32**-based device covers the visible light region with 400–700 nm, realizing better sunlight-style white emission where the EL spectra contain two main peaks located at 420 nm and 520 nm in keeping with the PL spectra, and CIE coordinates are located at (0.32, 0.31) (inset Fig. 6d) and the maximum CRI value reach 91. In addition, as you can see from the Fig. S11 in ESI,† the first emission peak at 420 and the shoulder peak at 445 nm are corresponding to the emission peak of **PFCz**, and the emission peak at 523 nm is assigned to the combination of the emission peak of **(CzhPI)$_2$Ir(fpptz)** at 508 nm and **Ir(piq)$_2$acac** at 613 nm. This feature is well explained in Fig. S12 in ESI,† it is obvious that the emission of polymer **PFCz** and the absorption spectrum of the Ir complexes show good spectra overlap. Therefore, efficient FRET from the **PFCz** to the Ir complex, and white-light emission can be expected by the combination of blue light-emitting from **PFCz** and green light-emitting from **(CzhPI)$_2$Ir(fpptz)** and red light-emitting from **Ir(piq)$_2$acac** through finely adjusting the content of Ir complex.

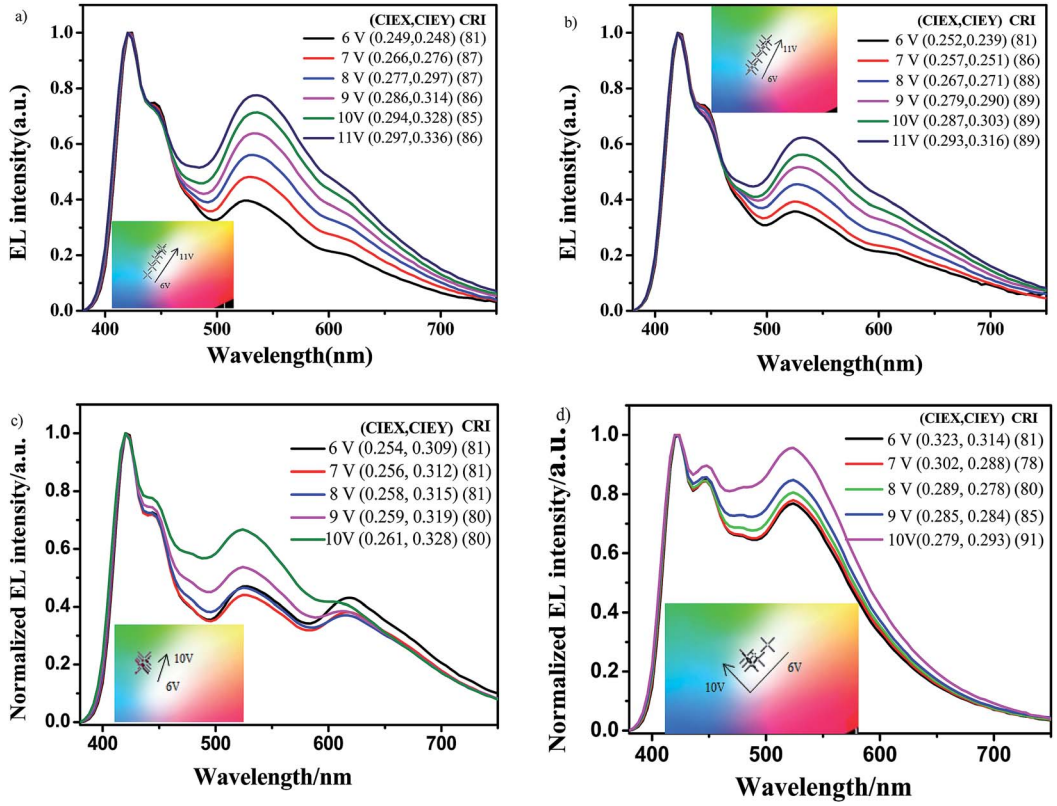

Fig. 6 Electroluminescence spectra and CIE coordinates (inset) of the hyperbranched polymers PLEDs: (a) **PFCzSDF10R8G8**, (b) **PFCzSDF10R8G16**, (c) **PFCzSDF10R8G24** and (d) **PFCzSDF10R8G32**.

Table 3 EL Performances of the PLEDs

Copolymer	V_{on}[a] (V)	L_{max}[b] (cd m^{-2}) (at the voltage (V))	CE_{max} (cd A^{-1})	LE_{max} (lm W^{-1})	CIE[c] (x, y)	CRI[c]	CCT[c]
PFCzSDF10R8G8	4.20	5548 (9.6)	0.89	0.32	(0.294, 0.328)	85	7598.80
PFCzSDF10R8G16	5.70	6048 (11.7)	1.97	0.68	(0.287, 0.303)	89	7669.6
PFCzSDF10R8G24	4.79	7326 (9.0)	3.59	1.87	(0.261, 0.328)	80	10 666.2
PFCzSDF10R8G32	4.50	9054 (8.4)	2.58	1.14	(0.323, 0.314)	81	10 369.8

[a] Turn-on voltage (at 1 cd m^{-2}). [b] Maximum luminance at applied voltage. [c] CIE, CRI and CCT values measured at a voltage of 10 V for devices a–c and at 6 V for devices d.

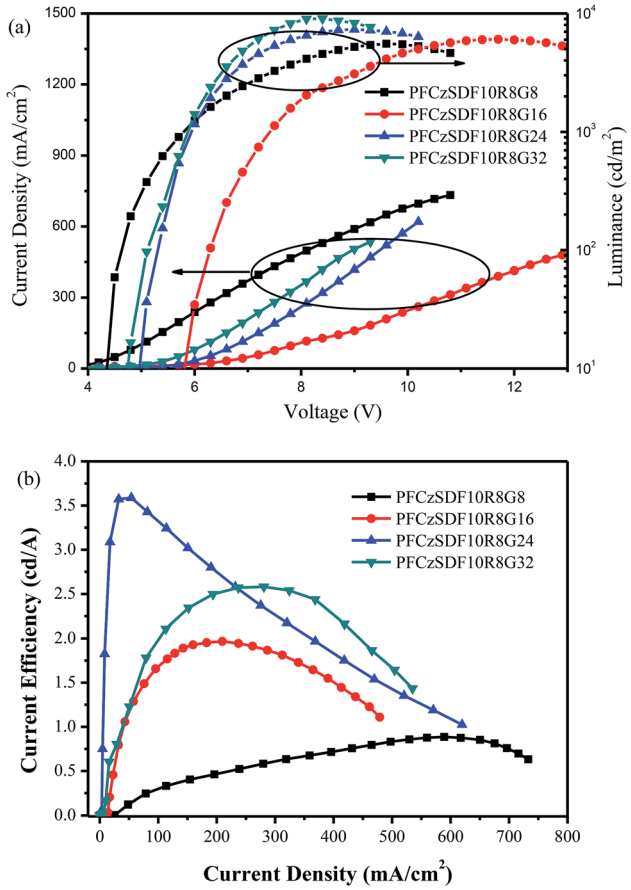

Fig. 7 Current density–voltage–brightness (*J*–*V*–*L*) curves characteristics (a) and current efficiency–current density characteristics (b) of hyperbranched polymers PLEDs.

The good EL spectra verified that förster energy transfer with intra- and interchain interaction from host **PFCz** segment to **(CzhBrPI)$_2$Ir(fpptz)** unit to **Ir(Brpiq)$_2$acac** unit again, and charge trapping effect simultaneously happen under high voltage in all hyperbranched polymers. Pure white-light emission was obtained for **PFCzSDF10R8G32** from the blue-light emitting of **PFCz** segment, the green-light emitting of **(CzhBrPI)$_2$Ir(fpptz)** and the complementary red-light emitting from **Ir(piq)$_2$acac** through both incomplete intra-, interchain FRET and the charge trapping processes. This is because that electrons and holes are readily trapped on the Ir complex after the injection of the electrons from the cathode and the holes from anode in the device under electrical excitation. In other words, the intra-, interchain FRET from **PFCz** unit to **(CzhPI)$_2$Ir(fpptz)** and **Ir(piq)$_2$acac** and the charge trapping of **(CzhPI)$_2$Ir(fpptz)** and **Ir(piq)$_2$acac** exist simultaneously in the electroluminescence process, and the charge trapping is more efficient under higher voltage. For all hyperbranched polymers-based OLEDs, the CRI values are greater than 80.

Fig. 7a shows the current density–voltage–brightness (*J*–*V*–*L*) characteristics of all devices. All devices exhibit moderate low turn-on voltage of 4.2–5.7 V (Table 3), which can be attributed to the small energy barrier between PEDOT:PSS and EML. The maximum luminance (~9054 cd m^{-2}) for the **PFCzSDF10R8G32**-based device is obtained. However its current efficiency (~2.58 cd A^{-1}) is less than the maximum current efficiency (~3.59 cd A^{-1}) of the **PFCzSDF10R8G24**-based device showing a maximum luminance of 7326 cd m^{-2}. This may be mainly due to the imbalance of carrier injection. As can be seen from Fig. 7b, the efficiencies decrease quite slowly with increasing current density, suggesting that these hyperbranched polymers and their devices have good stabilities. Further investigations on the optimization of the device performance and the synthesis of hyperbranched polymers with different structure and color groups are ongoing in our laboratory.

Conclusions

In conclusion, a series of hyperbranched polymers with 3,6-carbazole-*alt*-2,7-fluorene as the branches and the three-dimensional structured spiro[3,3]heptane-2,6-dispirofluorene (**SDF**, 10 mol%) as the core were prepared by Suzuki polycondensation with broad full width at half maximum bis(2-(4-bromophenyl)-1-[6-(9-carbazolyl)hexyl]-imidazole)(2-(5-(4-fluorinatedphenyl)-1,3,4-triazole)pyridine)iridium(III) (**(CzhBrPI)$_2$Ir(fpptz)**) and bis(1-phenyl-isoquinoline)(acetylacetonato) iridium(III) **(Ir(piq)$_2$acac)** as terminal adjusting light groups. The hyperbranched structures suppress the interchain interactions efficiently, and help to form amorphous spin-coating films. The FRET efficiency from **PFCz** segments to **(CzhBrPI)$_2$Ir(fpptz)** unit to **Ir(Brpiq)$_2$acac** unit again is remained in the hyperbranched systems. With the introduction of green light moiety **(CzhBrPI)$_2$Ir(fpptz)** into the polymers, the LUMO energy levels of polymers were also reduced to decrease the barrier for electron injection from the work function of LiF/Al (−2.9 eV) to EML in the PLEDs. Thus, the hyperbranched polymers exhibit good EL properties with the maximum luminance of 9054 cd m^{-2} (at

8.4 V), maximum current efficiency of 3.59 cd A^{-1} and the maximum CRI value reach 91. All hyperbranched polymer devices realized good white light emission, and the **PFCzSDF10R8G32**-based device achieved sunlight-style white light emission with CIE coordinates of (0.323, 0.314). The results indicate that the hyperbranched polymers introducing the green and red phosphor light groups having the broad full width at half maximum as the adjust spectral groups is promising candidates.

Conflicts of interest

The authors declare no competing financial interest.

Acknowledgements

The authors are grateful to the National Natural Science Foundation of China (61705158, 61605138, 61605137, 61775155, 61705156), Shanxi Province Natural Science Foundation (201601D202030, 201601D021018, 201601D011031, 201801D221102); and Scientific and Technological Innovation Programs of Higher Education Institutions in Shanxi (2016134, 2016135, 201802111).

Notes and references

1 T. Guo, L. Yu, B. Zhao, Y. Li, Y. Tao, W. Yang, Q. Hou, H. Wu and Y. Cao, *Macromol. Chem. Phys.*, 2012, **213**, 820–828.
2 F. Liu, J. Q. Liu, R. R. Liu, X. Y. Hou, L. H. Xie, H. B. Wu, C. Tang, W. Wei, Y. Cao and W. Huang, *J. Polym. Sci., Part A: Polym. Chem.*, 2009, **47**, 6451–6462.
3 W. B. Wu, S. H. Ye, L. J. Huang, L. Xiao, Y. J. Fu, Q. Huang, G. Yu, Y. Q. Liu, J. G. Qin, Q. Q. Li and Z. Li, *J. Mater. Chem.*, 2012, **22**, 6374–6382.
4 A. Pfaff and A. H. E. Müller, *Macromolecules*, 2011, **44**, 1266–1272.
5 P. Tao, Y. Q. Miao, H. Wang, B. S. Xu and Q. Zhao, *Chem. Rec.*, 2018, **18**, 1–32.
6 X. Wen, D. X. Zhang, T. C. Ren, J. C. Xiao, Y. G. Wu, L. B. Bai and X. W. Ba, *Dyes Pigm.*, 2017, **137**, 437–444.
7 T. Guo, R. Guan, J. Zou, J. Liu, L. Ying, W. Yang, H. Wu and Y. Cao, *Polym. Chem.*, 2011, **2**, 2193–2203.
8 R. Guan, Y. Xu, L. Ying, W. Yang, H. Wu, Q. Chen and Y. Cao, *J. Mater. Chem.*, 2009, **19**, 531–537.
9 J. Liu, L. Yu, C. Zhong, R. He, W. Yang, H. Wu and Y. Cao, *RSC Adv.*, 2012, **2**, 689–696.
10 N. K. Geitner, B. Wang, R. E. Andorfer, D. A. Ladner, P. C. Ke and F. Ding, *Environ. Sci. Technol.*, 2014, **48**, 12868–12875.
11 Y. T. Tsai, C. T. Lai, R. H. Chien, J. L. Hong and A. C. Yeh, *J. Polym. Sci., Part A: Polym. Chem.*, 2012, **50**, 237–249.
12 R. Wang, W. Z. Wang, G. Z. Yang, T. Liu, J. Yu and Y. Jiang, *J. Polym. Sci., Part A: Polym. Chem.*, 2008, **46**, 790–802.
13 J. Y. Chen, M. Smet, J. C. Zhang, W. K. Shao, X. Li, K. Zhang, Y. Fu, Y. H. Jiao, T. Sun, W. Dehaen, F. C. Liud and E. H. Han, *Polym. Chem.*, 2014, **5**, 2401–2410.
14 L. R. Tsai and Y. Chen, *J. Polym. Sci., Part A: Polym. Chem.*, 2007, **45**, 4465–4476.
15 C. He, L. W. Li, W. D. He, W. X. Jiang and C. Wu, *Macromolecules*, 2011, **44**, 6233–6236.
16 D. Konkolewicz, C. K. Poon, A. Gray-Weale and S. Perrier, *Chem. Commun.*, 2011, **47**, 239–241.
17 L. R. Tsai and Y. Chen, *Macromolecules*, 2008, **41**, 5098–5106.
18 M. C. Gather, A. Kohnen and K. Meerholz, *Adv. Mater.*, 2011, **23**, 233–248.
19 J. Liu, Y. Cheng, Z. Xie, Y. Geng, L. Wang, X. Jing and F. Wang, *Adv. Mater.*, 2008, **20**, 1357–1362.
20 Y. Q. Miao, K. X. Wang, L. Gao, B. Zhao, Z. Q. Wang, Y. P. Zhao, A. Q. Zhang, H. Wang, Y. Y. Hao and B. S. Xu, *J. Mater. Chem. C*, 2018, **6**, 1853–1862.
21 L. Ying, C. L. Ho, H. Wu, Y. Cao and W. Y. Wong, *Adv. Mater.*, 2014, **26**, 2459–2473.
22 Y. Q. Miao, K. X. Wang, L. Gao, B. Zhao, H. Wang, F. R. Zhu, B. S. Xu and D. G. Ma, *J. Mater. Chem. C*, 2018, **6**, 8122–8134.
23 Z. Wang, J. Zhou and J. Wang, *IEEE Access*, 2019, **7**, 29520–29532.
24 B. H. Zhang, G. P. Tan, C. S. Lam, B. Yao, C. L. Ho, L. H. Liu, Z. Y. Xie, W. Y. Wong, J. Q. Ding and L. X. Wang, *Adv. Mater.*, 2012, **24**, 1873–1877.
25 Y. Q. Miao, K. X. Wang, B. Zhao, L. Gao, P. Tao, X. G. Liu, Y. Y. Hao, H. Wang, B. S. Xu and F. R. Zhu, *Nanophotonics*, 2018, **7**, 295–304.
26 W. Yang, X. M. Wang, S. N. Wang and W. T. Hao, *J. Appl. Polym. Sci.*, 2018, **135**, 46015.
27 J. Sun, D. Y. Wu, L. Gao, M. N. Hou, G. J. Lu, J. Li, X. W. Zhang, Y. Q. Miao, H. Wang and B. S. Xu, *RSC Adv.*, 2018, **8**, 1638–1646.
28 Y. D. Jiu, J. Y. Wang, C. F. Liu, W. Y. Lai, L. L. Zhao, X. C. Li, Y. Jiang, W. D. Xu, X. W. Zhang and W. Huang, *Chin. J. Chem.*, 2015, **33**, 873–880.
29 W. Bernal, A. Barbosa-García, A. Aguilar-Granda, E. Pérez-Gutiérrez, J. L. Maldonado, M. J. Percino and B. Rodríguez-Molina, *Dyes Pigm.*, 2019, **163**, 754–760.
30 J. Peng, W. L. Yu, W. Huang and H. Alan, *Adv. Mater.*, 2000, **12**, 828.
31 Y. L. Wu, J. Li, W. Q. Liang, J. L. Yang, J. Sun, H. Wang, X. G. Liu, B. S. Xu and W. Huang, *RSC Adv.*, 2015, **5**, 49662–49670.
32 S. Q. Yu, H. Y. Lin, Z. J. Zhao, Z. X. Wang and P. Lu, *Tetrahedron Lett.*, 2007, **48**, 9112–9115.
33 O. P. Y. Moll, T. Le Borgne, P. Thuéry and M. Ephritikhine, *Tetrahedron Lett.*, 2001, **42**, 3855–3856.
34 J. W. Kim, S. H. Kim, J. Kim, I. Kim, Y. G. Jin, J. H. Kim, H. Y. Woo, K. Lee and H. S. Suh, *Macromol. Res.*, 2011, **19**, 589–598.
35 H. Wang, J. T. Ryu and Y. Kwon, *J. Appl. Polym. Sci.*, 2011, **119**, 377–386.
36 Y. Li, Y. Liu and M. Zhou, *Dalton Trans.*, 2012, **41**, 3807–3816.
37 J. Qiao, L. Duan, L. Tang, L. He, L. Wang and Y. Qiu, *J. Mater. Chem.*, 2009, **19**, 6573.
38 L. Duan, L. Hou, T. W. Lee, J. Qiao, D. Zhang, G. Dong, L. Wang and Y. Qiu, *J. Mater. Chem.*, 2010, **20**, 6392.
39 T. Sudyoadsuk, P. Moonsin, N. Prachumrak, S. Namuangruk, S. Jungsuttiwong, T. Keawin and V. Promarak, *Polym. Chem.*, 2014, **5**, 3982–3993.

40 Y. N. Li, J. F. Ding, M. Day, Y. Tao, J. P. Lu and M. D'iorio, *Chem. Mater.*, 2004, **16**, 2165–2173.
41 Y. L. Wu, J. Li, W. Q. Liang, J. L. Yang, J. Sun, H. Wang, X. G. Liu, B. S. Xu and W. Huang, *New J. Chem.*, 2015, **39**, 5977.
42 T. Guo, L. Yu, Y. Yang, Y. H. Li, Y. Tao, Q. Hou, L. Ying, W. Yang, H. B. Wu and Y. Cao, *J. Lumin.*, 2015, **167**, 179–185.
43 T. Guo, L. Yu, B. F. Zhao, L. Ying, H. B. Wu, W. Yang and Y. Cao, *J. Polym. Sci., Part A: Polym. Chem.*, 2015, **53**, 1043–1051.
44 H. Wang, Y. Xu, T. Tsuboi, H. Xu, Y. Wu, Z. Zhang, Y. Miao, Y. Hao, X. Liu, B. Xu and W. Huang, *Org. Electron.*, 2013, **14**, 827–838.
45 J. Yang, C. Y. Jiang, Y. Zhang, R. Q. Yang, W. Yang, Q. Hou and Y. Cao, *Macromolecules*, 2004, **37**, 1211–1218.
46 Z. M. Wang, P. Lu, S. F. Xue, C. Gu, Y. Lv, Q. Zhu, H. Wang and Y. G. Ma, *Dyes Pigm.*, 2011, **91**, 356–363.